Journal of the Serbian Chemical Society
JSCS@tmf.bg.ac.rs • www.shd.org.rs/JSCS
J. Serb. Chem. Soc. 88 (7–8) S209–S213 (2023) *Supplementary material*

SUPPLEMENTARY MATERIAL TO

Investigating inhibition characteristics of *Butea monosperma* leaf extracts to retard stainless steel biocorrosion in the presence of sulfate-reducing bacteria

SHIV KUMAR MANU, NOYEL VICTORIA SELVAM
and MANIVANNAN RAMACHANDRAN*

Department of Chemical Engineering, National Institute of Technology Raipur, Chhattisgarh – 492010, India

J. Serb. Chem. Soc. 88 (7–8) (2023) 749–764

Fig. S-1a and b show the corrosion rate of SS 202 in modified Baar's medium containing with (I) and without (U) palash leaf extract in the absence of bacteria and inhibition efficiency as a function of immersion time respectively. From Fig. 1a and S-1, it is clear that the corrosion rate in the abiotic case is significantly less when compared with the biotic case for both uninhibited and inhibited samples. The corrosion inhibition efficiency decreases with an increase in the immersion period, as seen in Fig. S-1b.

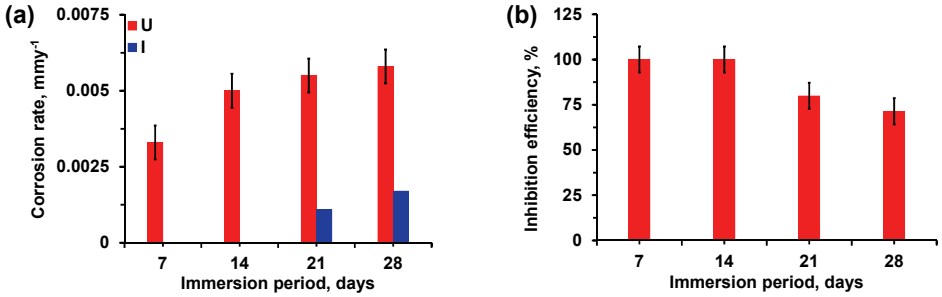

Fig. S-1. (a) Corrosion rate of stainless steel immersed in U and I medium in the absence of bacteria and (b) inhibition efficiency as a function of immersion period.

From Fig. S-2, after the supplementation of the PLE, a decrease in dissolved sulfide content is clearly seen. This shows that the extract affects the metabolic activity of the bacteria resulting in reduced dissolved sulfide concentration. The sulfide content in the UB sample increased from 48 ppm in the first week to 69 ppm in the fourth week. On the other hand, the IB sample showed a continuously

* Corresponding author. E-mail: rmani.che@nitrr.ac.in

decreasing trend in the sulfide values which ultimately goes to zero in the fourth week.

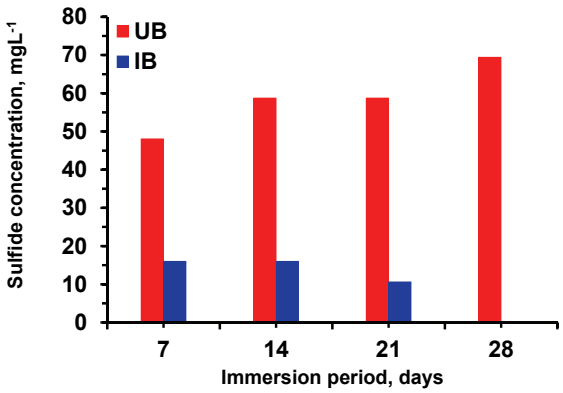

Fig. S-2. Effect of immersion time on dissolved sulfide concentrations for SS 202 in UB and IB medium.

Fig. S-3a and b show the impedance modulus measured at different frequencies in UB and IB samples at varied immersion times. Fig. S-3c and d show the phase angle variations with frequency for the same. From Fig. S-3a and c, it can be noticed that the addition of the inhibitor extract increases the impedance modulus approximately by ten times. The impedance modulus at low frequency for the UB sample decreases significantly during the third week and increases to a greater extent in the fourth week. This is due to the development of a thicker corrosion products film during the fourth week which prevents the movement of the electrolyte. In the case of IB samples, the maximum impedance modulus at low frequency is observed for the third week. This decreases again in the fourth week which is due to the change in the thickness and composition of the external film formed on the metal. The formation of a thicker corrosion products layer during third week in IB sample matches well with the SEM findings. Overall, the impedance modulus of the IB samples is approximately ten-times higher at low frequencies for all the immersion durations indicating higher resistance to material degradation. The Bode phase angle plot shows the presence of two-time constants in both cases. In the case of UB samples, the phase angle at the lowest frequency decreases for the second and third weeks indicating an increase in corrosion. For the fourth week, the low-frequency peak is broader and shows a shift towards low frequency which indicates good adsorption of the external film on the metal surface which offers protection against corrosion.[1]

In the case of IB samples, the phase angle peak at low frequency increases slightly for the second week. For the third week, the phase angle peak at the

lower frequency region is much broader when compared to other weeks. The impedance modulus plot for the same period shows a maximum value at the lowest frequency which indicates that the film formed during the third week is continuous with good corrosion protection. Similarly, for the fourth week, the phase angle peak shows a shift towards lower frequency accompanied by an increase in peak value indicating good corrosion protection with immersion time.[1]

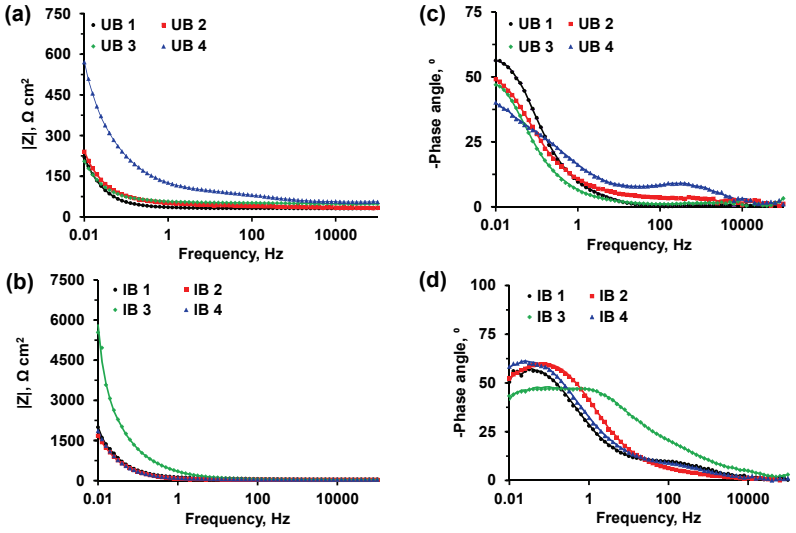

Fig. S-3. Bode impedance modulus for SS 202 in (a) UB and (b) IB medium at different immersion periods. Bode phase angle plot for SS 202 in (c) UB and (d) IB medium at different immersion periods.

Tafel plot for the SS sample in UB and IB media after immersion for defined durations is shown in Fig. S-4. The Tafel parameters obtained after Tafel region extrapolation are listed in Table II. It can be seen that the E_{corr} shows a positive shift with the immersion period in both UB and IB samples. This shows the formation of passive layer which prevents the diffusion of the corrosive medium. With the inhibitor addition, a significant negative shift in E_{corr} is observed for the first week which could be attributed to the decreased hydrogen generation at the cathode due to the adsorption of the inhibitor molecules.[2] From the second week positive shift in the potential with inhibitor addition can be observed. Moreover, it is clearly observed that both the cathodic and the anodic current densities are drastically decreased with the inhibitor addition. This gives information that both the cathodic hydrogen generation and anodic dissolution reactions are affected with the inhibitor addition. Thus, the inhibitor acts as a mixed inhibitor.

Previously, the sulfide analysis results indicated that the inhibitor affected the metabolic activities of the SRB. Thus, the inhibitor works as a corrosion inhibitor and also as an antibacterial agent. Moreover, the j_{corr} values are lowered with the addition of the inhibitor for all weeks and with immersion time it shows a continuously decreasing trend which shows the improved corrosion resistance properties of the inhibitor layer with time. In the absence of the inhibitor continuously increasing trend in the same can be observed. On the other hand, a continuously decreasing tendency is observed for j_{corr} with the inhibitor extract.

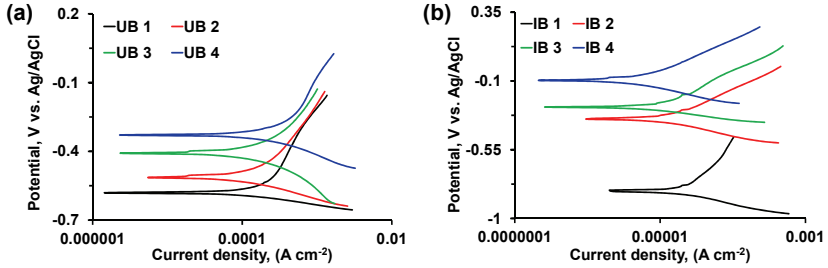

Fig. S-4. Polarization plots for SS 202 coupons immersed in (a) UB (b) IB media at four immersion periods.

Table S-I shows the elemental composition of the UB and IB samples at different immersion period. The IB samples show higher carbon content when compared to UB samples which could be due to the adsorbed inhibitor molecules. The sulfide and iron concentrations are high in the UB samples due to the formation and deposition of iron sulfide.

TABLE S-I. Elemental analyses of the layer formed on the stainless-steel coupons immersed in UB and IB medium for 1- and 3-week immersion periods. All values are in at. %

Element	UB 1	UB 3	IB 1	IB 3
C	30.40	33.49	70.18	70.74
O	48.07	37.85	20.60	20.22
Na	0.60	1.56	0.02	0
Mg	1.57	1.86	0	0.03
Si	0.06	0.83	0.44	0.63
P	5.19	6.12	8.13	7.77
S	3.14	3.33	0.18	0.10
Ca	7.00	3.80	0.21	0.33
Cr	0.04	1.13	0.06	0
Mn	1.81	0.49	0.02	0.03
Fe	1.80	9.02	0.16	0.05
Ni	0.06	0.05	0	0.12
Cu	0.27	0.46	0	0

The findings of the GC-MS analysis of PLE are given in Table S-II. The analysis shows that about 78.9 % of the extract is composed of terpenoids which

are known for their antioxidant and antibacterial properties. Similarly, compounds such as vitamin-E and W-18 are also helpful in controlling bacterial growth and corrosion.

TABLE S-II. List of few compounds present in significant quantities in palash leaf extract identified from GC-MS analysis

Compound name	Time (min)	Area (%)	Group
3-O-Methyl-d-glucose	20.49	3.22	D-aldohexose
Hexadecanoic acid, 2-hydroxy-1-(hydroxymethyl)ethyl ester	37.97	3.33	Ester
Di(pentamethylphenyl)ketone	44.08	6.20	Ketones
W-18	44.70	3.79	Opioid
Vitamin E	46.80	4.53	Methylated phenol
Lup-20(29)-en-3-one	49.85	40.95	Triterpenoid
Betulin	50.14	19.79	Pentacyclic triterpenoid
γ-Sitostenone	50.99	18.20	Tetracyclic terpene

REFERENCES

1. S. Meng, Z. Liu, X. Zhao, B. Fan, H. Liu, M. Guo, H. Hao, *RSC Adv.* **11** (2021) 31693 (https://doi.org/10.1039/d1ra04976c)
2. A. Kumar, P.C. Srivastava, *Mater. Sci.-Pol.* **37** (2019) 116 (https://doi.org/10.2478/msp-2019-0001).